Relationships between global precipitation and surface temperature on interannual and longer timescales (1979–2006)

Robert F. Adler,[1,2] Guojun Gu,[2,3] Jian-Jian Wang,[2,3] George J. Huffman,[2,4] Scott Curtis,[5] and David Bolvin[2,4]

Received 3 June 2008; revised 9 September 2008; accepted 25 September 2008; published 20 November 2008.

[1] Associations between global and regional precipitation and surface temperature anomalies on interannual and longer timescales are explored for the period of 1979–2006 using the GPCP precipitation product and the NASA-GISS surface temperature data set. Positive (negative) correlations are generally confirmed between these two variables over tropical oceans (lands). ENSO is the dominant factor in these interannual tropical relations. Away from the tropics, particularly in the Northern Hemisphere mid-high latitudes, this correlation relationship becomes much more complicated with positive and negative values of correlation tending to appear over both ocean and land, with a strong seasonal variation in the correlation patterns. Relationships between long-term linear changes in global precipitation and surface temperature are also assessed. Most intense long-term, linear changes in annual-mean rainfall during the data record tend to be within the tropics. For surface temperature however, the strongest linear changes are observed in the Northern Hemisphere mid-high latitudes, with much weaker temperature changes in the tropical region and Southern Hemisphere. Finally, the ratios between the linear changes in zonal-mean rainfall and temperature anomalies over the period are estimated. Globally, the calculation results in a +2.3%/°C precipitation change, although the magnitude is sensitive to small errors in the precipitation data set and to the length of record used for the calculation. The long-term temperature-precipitation relations are also compared to the interannual variations of the same ratio in a zonally averaged sense and are shown to have similar profiles, except for over tropical land areas.

Citation: Adler, R. F., G. Gu, J.-J. Wang, G. J. Huffman, S. Curtis, and D. Bolvin (2008), Relationships between global precipitation and surface temperature on interannual and longer timescales (1979–2006), *J. Geophys. Res.*, *113*, D22104, doi:10.1029/2008JD010536.

1. Introduction

[2] Understanding and exploring the interannual and interdecadal/longer-term variability in the global energy and hydrological (water) cycle is an essential part of the task of assessing global climate variability and possible change. In particular, we need to quantify how the entire energy and water cycle, especially the two key components of surface precipitation and temperature may respond to various internal and external climate forcings on interannual and longer timescales [e.g., *Trenberth et al.*, 1998; *Robock*, 2000; *Wigley*, 2000; *Mantua and Hare*, 2002; *Soden et al.*, 2002; *van Loon et al.*, 2004; *Allan and Soden*, 2007].

[3] On the interannual timescale, the ENSO dominates climate variability in the Tropics and effectively extends its effect to the mid-high latitudes [e.g., *Trenberth et al.*, 1998, 2002; *Wigley*, 2000; *Curtis and Adler*, 2003; *Smith et al.*, 2006]. ENSO can cause significant temperature anomalies and simultaneously shift the major rainy zones across the low latitudes, and further modulate precipitation and temperature anomalies beyond the Tropics [e.g., *Trenberth et al.*, 1998, 2002; *Dai and Wigley*, 2000; *Curtis and Adler*, 2003]. At higher latitudes, through associated large-scale circulation anomalies, the Arctic Oscillation (AO) also induces precipitation and temperature changes at this timescale in the Northern Hemisphere, especially in the mid-higher latitudes [*Thompson and Wallace*, 1998]. The same may also be true for the Antarctic Oscillation (AAO). Large volcanic eruptions are another known natural factor that may cause significant anomalies in both surface temperature and precipitation through affecting incoming solar radiation and microphysical processes in clouds [e.g., *Robock*, 2000; *Gillett et al.*, 2004; *Gu et al.*, 2007]. On the interannual timescale both global precipitation and surface temperature data sets can be used to diagnose variations with a high degree of confidence.

[1]Earth System Science Interdisciplinary Center, University of Maryland, College Park, Maryland, USA.
[2]Laboratory for Atmospheres, NASA Goddard Space Flight Center, Greenbelt, Maryland, USA.
[3]Goddard Earth Sciences and Technology Center, University of Maryland Baltimore County, Baltimore, Maryland, USA.
[4]Science Systems and Applications Inc, Lanham, Maryland, USA.
[5]Department of Geography, East Carolina University, Greenville, North Carolina, USA.

Copyright 2008 by the American Geophysical Union.
0148-0227/08/2008JD010536

[4] On longer timescales, positive surface temperature changes have been demonstrated to be a prominent phenomenon of the past decades, with increased, man-made greenhouse gases being a major reason [*IPCC*, 2007]. Regarding an associated global precipitation change, however, results are not as clear as for interannual variations. The Pacific Decadal Oscillation (PDO) and AO could also be linked to variations on this interdecadal/decadal timescale. Efforts have been made to examine long-term precipitation changes by means of both carefully setting up numerical simulations and analyzing the rain gauge–based land surface precipitation and currently available, satellite-based precipitation products [e.g., *Dai et al.*, 1997; *Yang et al.* [2003]; *Kumar et al.*, 2004; *Déry and Wood*, 2005; *Smith et al.*, 2006; *Gu et al.*, 2007; *Wentz et al.*, 2007; *Allan and Soden*, 2007]. Using the monthly rainfall product from the Global Precipitation Climatology Project (GPCP; *Adler et al.* [2003]), *Smith et al.* [2006] showed that there are probably tropical trend-like rainfall changes with spatial variations, and it was further proposed that these changes might be related to the interdecadal variability of tropical sea surface temperature (SST). *Gu et al.* [2007] examined the long-term rainfall changes also using the GPCP rainfall product and found significant increases in the annual-mean tropical total and oceanic rainfall, but a negligible, negative change in the annual-mean tropical land rainfall. The impacts of ENSO and volcanic eruptions during the GPCP record were also assessed in that study. *Allan and Soden* [2007] found positive (negative) trends in observed tropical precipitation in areas of ascending (descending) vertical motion, deduced from reanalysis models. Thus although there are indications of long-term rainfall changes occurring, we have less confidence in these precipitation increases than we do in the surface temperature increases, which seem to be on firm ground observationally. These results seem to be qualitatively in accord with diagnostic results of numerical outputs [e.g., *Yang et al.*, 2003; *Kumar et al.*, 2004]. Separately exploring changes in precipitation and surface temperature on longer-than-seasonal timescales is surely important. Quantifying the covariability relations between precipitation and temperature at these timescales is also essential to improve our knowledge of the processes, particularly regional responses, and on surface energy and water budgets. Variations in precipitation and surface temperature are closely associated because of their thermodynamic relations, such as latent heat transfer during phase-changes within clouds and across the Earth surface, water substances' radiative properties, which are important features of the energy and water cycle, and the spatial structure and variation of atmospheric stability. Past studies investigated the relationship between precipitation and temperature in various regions [e.g., *Madden and Williams*, 1978; *Isaac and Stuart*, 1992; *Zhao and Khalil*, 1993]. Regional and seasonal dependencies were evident. *Déry and Wood* [2005] quantified the covariability of these two variables over global land. Negative correlations between annual mean precipitation and temperature are often observed over tropical land, and part of the subtropics and midlatitudes, and significant positive correlations appear in the higher latitudes. The possible concurrent long-term/interdecadal changes in these two components over land were further examined. *Trenberth and Shea* [2005] explored the relationship between precipitation and temperature using data sets (the GPCP precipitation and ERA-40 air temperature) with global coverage, and compared them against model outputs. A contrasting temperature-precipitation relationship occurs over tropical land and ocean. Furthermore, a strong seasonal variation seems to appear in the Northern Hemisphere higher latitudes. These studies provide a basic account of the covariability in precipitation and temperature. However, detailed global patterns of, and physical mechanisms modulating this covariability are far from clear. A key question is that, given the dominance of interannual variability in linear correlation relationships between precipitation and temperature [e.g., *Trenberth and Shea*, 2005], whether a similar covariability exists at other timescales, specifically on the interdecadal/long-term timescale. Hence the purpose of this study is to explore the covariability in precipitation and temperature on both interannual and interdecadal/long-term timescales by means of two model-independent data sets: the GPCP monthly precipitation and the NASA-GISS surface temperature products. Because of a relatively short data record of precipitation, the variabilities on the interdecadal/long-term timescales discussed here likely include contributions from some known decadal modes, such as PDO and AO [*Gu et al.*, 2007].

[5] Section 2 briefly describes the two data sets. Results are presented in section 3, including global correlation analyses between precipitation and surface temperature anomalies primarily on the interannual timescale, and possible modulations by ENSO and AO. Also covered in this section are the estimates of the global long-term changes in both precipitation and temperature, and their possible associations.

2. Brief Description of Data

[6] The monthly precipitation product from the Global Precipitation Climatology Project (GPCP) is a community-based analysis of global precipitation under the auspices of the World Climate Research Program (WCRP) from 1979 to the present [*Adler et al.*, 2003]. Archived on a $2.5° \times 2.5°$ grid, the data are combined from various information sources: microwave-based estimates from Special Sensor Microwave/Imager (SSM/I), infrared (IR) rainfall estimates from geostationary and polar-orbiting satellites, and surface rain gauges. Though the data are homogeneous since 1988 in terms of input data sets, the satellite inputs are limited to infrared-based estimates during the pre-1988 period. However, these pre-1988 estimates are trained on the later period to reduce possible differences. Certainly we should be cautious of this time inhomogeneity in the analysis in terms of satellite input data sets, even though *Smith et al.* [2006] showed that the impact of this time inhomogeneity is not a major concern. Detailed procedures and input data information can be found in the study of *Adler et al.* [2003].

[7] The NASA-GISS monthly temperature product is on a $1° \times 1°$ grid, and primarily an anomaly field. It combines air temperature anomalies from meteorological station measurements over land with sea surface temperature (SST) [*Hansen et al.*, 1999]. The SST data set is retrieved from satellite measurements during the post-1981 period [*Reynolds et al.*, 2002]. Details can be found by the study of

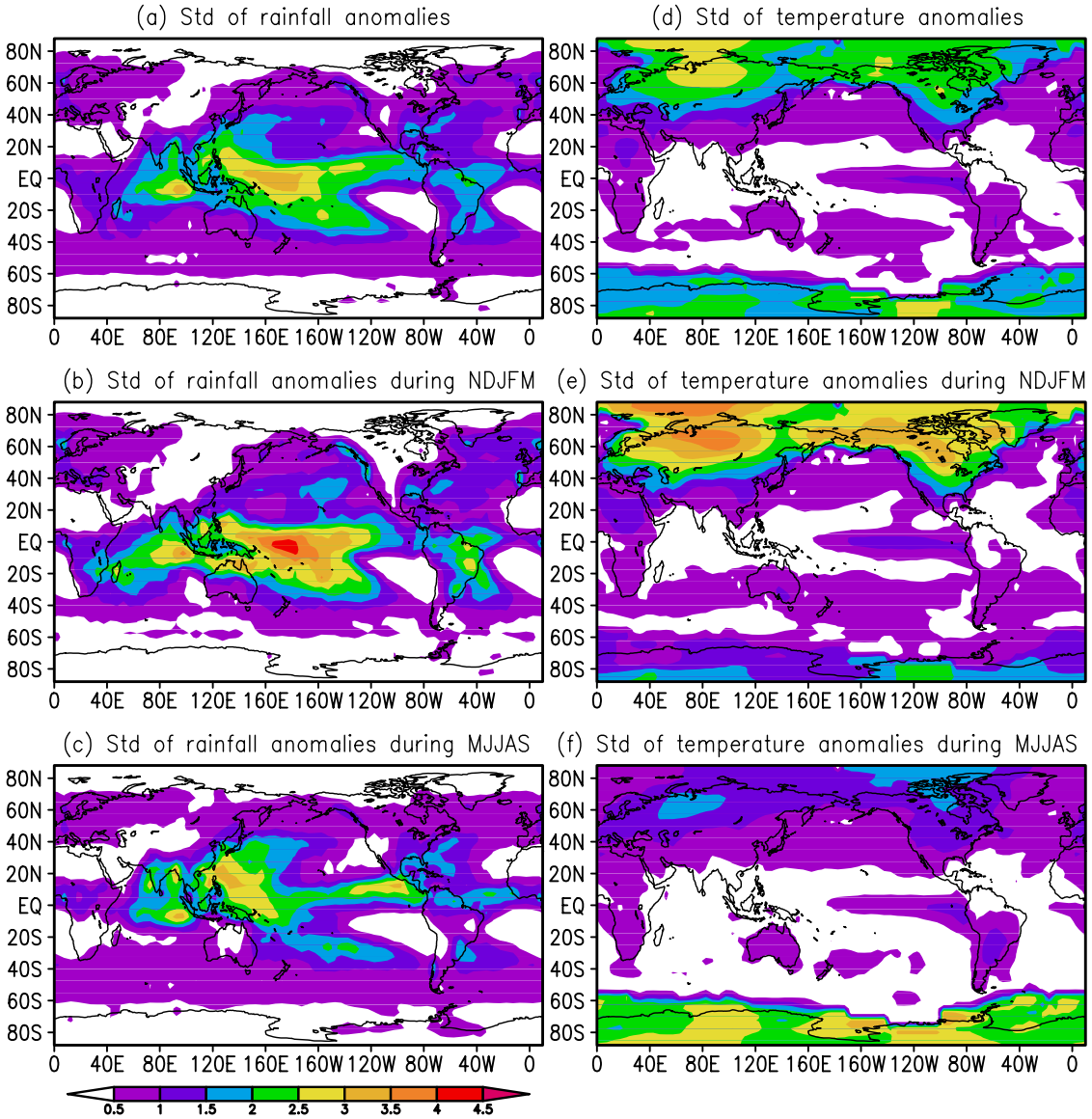

Figure 1. Standard deviations (Std) of monthly precipitation (mm day^{-1}; a, b, c) and surface temperature (°C; d, e, f) anomalies.

Hansen et al. [1999] and the product can be accessed through the NASA-GISS website.

[8] For easy comparison and for computation purposes, both data products are merged onto a same 5° × 5° grid.

3. Results

3.1. Global Features of Interannual Variations

[9] Before the linear correlations between precipitation and temperature are examined, their standard deviations are first computed to show their spatial distributions of variability (Figure 1). As in the study of *Trenberth and Shea* [2005], the most intense rainfall changes are observed in the Tropics, particularly over the tropical ocean. In contrast, the prominent variability in surface temperature is located in the higher latitudes and mostly over land. The strong interannual temperature changes in the tropics are primarily focused on two regions: one is located in the tropical central-eastern Pacific, corresponding to the El Niño/La Niña region, and another over the African deserts.

[10] Seasonal variations of the standard deviations are evident. More intense rainfall variations occur during November–March (NDJFM). And particularly, it seems that precipitation and temperature variability in the Northern Hemisphere mid-higher latitudes is stronger during NDJFM than during May–September (MJJAS) due to greater dynamical activity and tighter temperature gradients. During MJJAS, more intense temperature changes are seen south of 60°S. Also, temperature changes in the ENSO activity region are stronger during NDJFM, indicating a seasonal preference for the ENSO events [e.g., *Rasmusson and Carpenter*, 1982].

[11] Linear correlations between monthly precipitation and surface temperature anomalies for all months during 1979–2006 are shown in Figure 2a (Figure 2 shows the detrended correlation features, although the linear changes

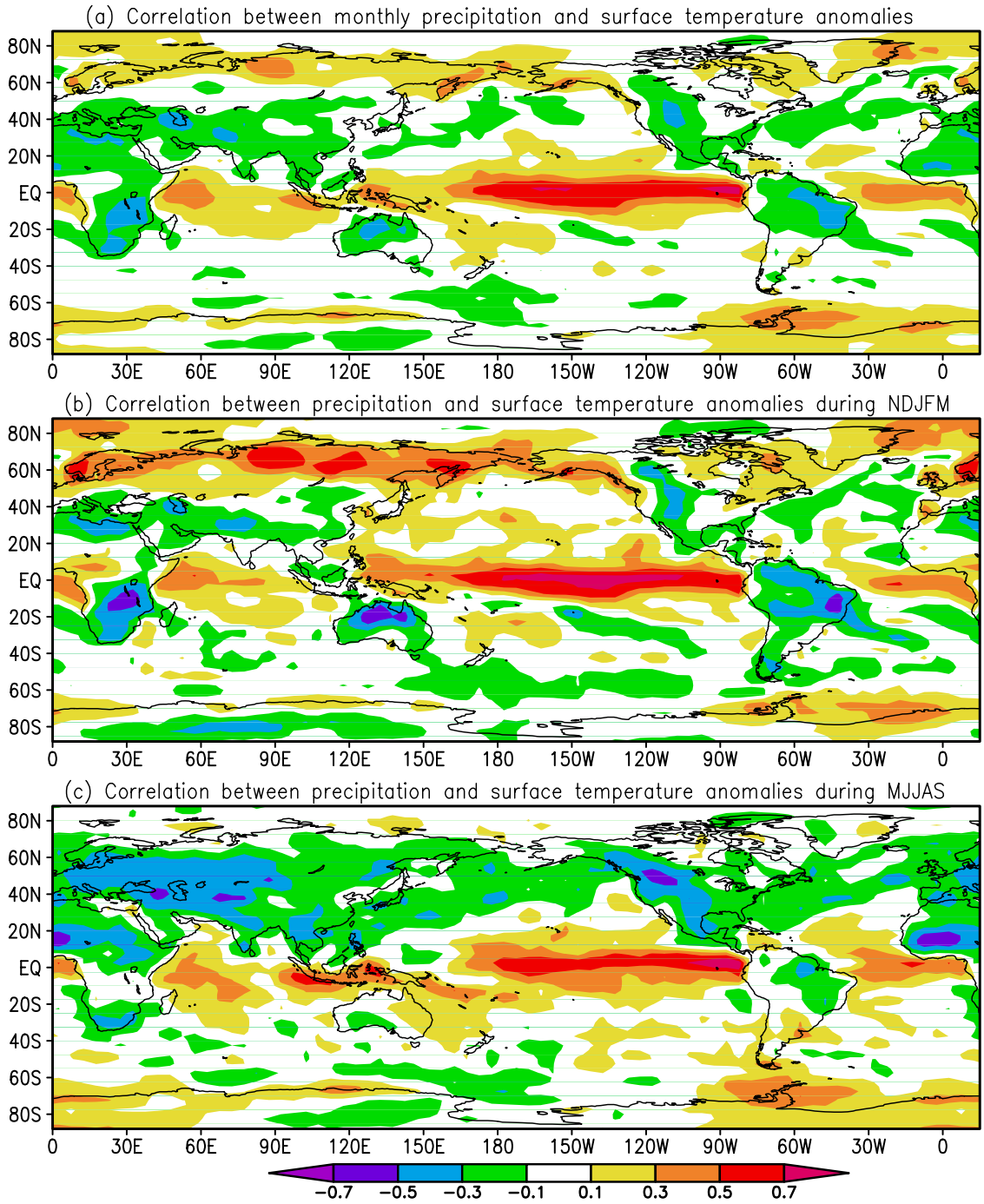

Figure 2. Correlations between monthly precipitation and surface temperature anomalies during (a) all months, (b) November–March (NDJFM), and (c) May–September (MJJAS). The local 5% confidence levels are about ±0.20 (for a) and ±0.25 (for b and c) after temporal autocorrelations are considered.

in both fields only have very limited effects, and the linear correlations are dominated by interannual variability in both fields (see Figure 5).). The local confidence levels of correlation are also estimated through applying a two-tailed significance test and estimating the decorrelation timescales at grid points [e.g., *Livezey and Chen*, 1983]. In the Tropics (25°S–25°N), positive correlation dominates over oceans, whereas significant, negative correlations appear over land. This contrasting feature likely implies the dominance of oceanic forcing in the tropical region, and opposite effects over land and ocean [e.g., *Trenberth et al.*, 1998, 2002; *Gu et al.*, 2007]. Increased surface temperature over oceans produces increased water vapor and increased precipitation. Over land subsidence (rising motion) due to ENSO or other effects compensating for events over the ocean produces warming (cooling), decreased humidity (increased humidity

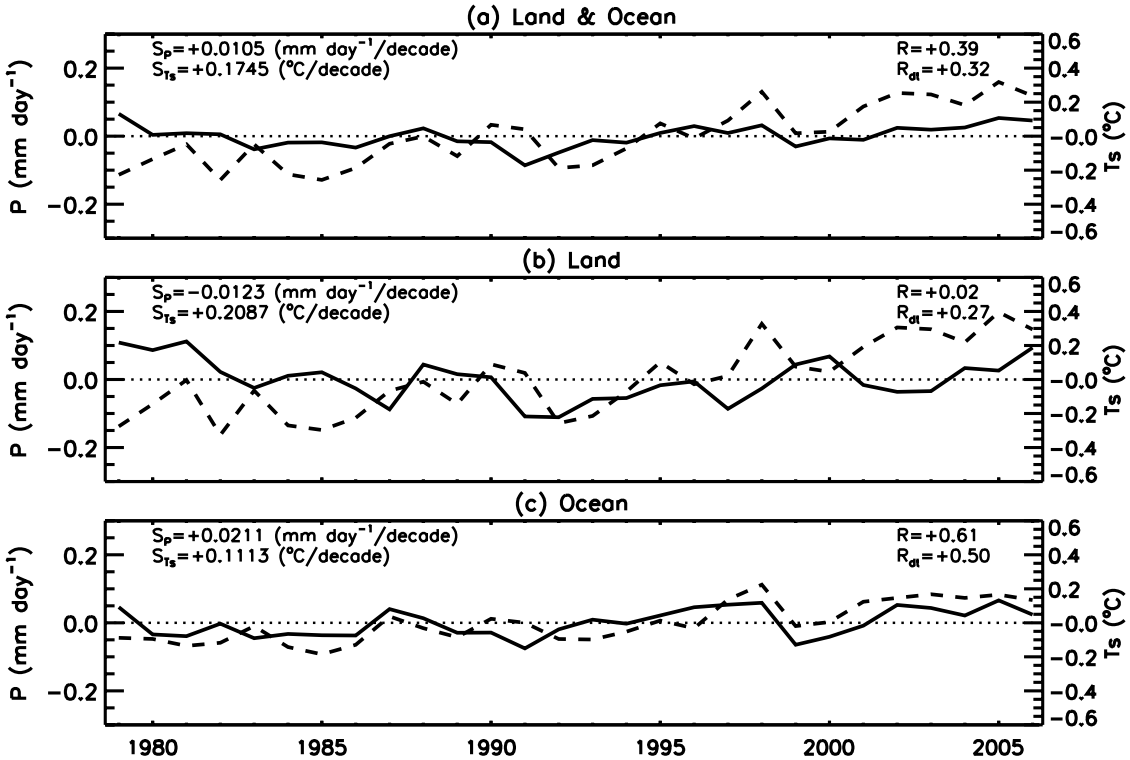

Figure 3. Correlations between zonal mean monthly rainfall and surface temperature anomalies with (solid) and without (dashed) long-term linear changes. The 5% and 1% confidence levels for correlation coefficient are 0.39 and 0.50, respectively, based on the degrees of freedom (dof) = 24, which is roughly estimated from the lag-one autocorrelations.

and cloudiness), and less (more) rainfall. Negative correlations are observed in the Northern Hemisphere midlatitudes (roughly 20°–45°N), particularly over land, probably related to variations in mean monthly positions of large-scale waves and pressure centers with their associated patterns of ascent/rain/cooling and descent/drying/warming. However, positive correlations dominate north of 50°N, where at lower mean temperatures a positive temperature anomaly is associated with increased moisture, clouds and precipitation. The correlation between precipitation and temperature in the Southern Hemisphere tends to be weaker than in the Northern Hemisphere. South of about 40°S, strong correlations are only seen in several places scattered along the coast of the Antarctic Continent.

[12] The correlations are further estimated for two distinct seasons: NDJFM and MJJAS (Figures 2b and 2c). Similar features are observed in the Tropics during these two seasons but the magnitudes of correlation are different. Much stronger, positive correlations occur in the tropical Pacific during NDJFM, reflecting the seasonal phase-locking of the ENSO events. Comparable features are seen in the two other major ocean basins: tropical Indian and Atlantic Oceans. Over land, negative correlations are much stronger during NDJFM as compared to MJJAS in southern Africa, Australia, and South America, again reflecting stronger ENSO activity in this season. One exception is over West Africa where stronger, negative correlations appear during MJJAS. Also, in the Maritime Continent where evident positive correlation occurs during MJJAS while weaker, positive and even negative correlations appear during NDJFM. These features are generally consistent with *Trenberth and Shea* [2005] with an exception in the tropical western Pacific region. They showed strong negative correlation in this region particularly during MJJAS, and ascribed it to the modulation of ENSO. However, only weak, negative correlation is seen in Figure 2c and it is concentrated in a much smaller domain. This tends to suggest a combined consequence of local SST forcing and the remote ENSO modulation.

[13] Seasonal changes in correlation are even more evident in the Northern Hemisphere mid-to-higher latitudes. Strong negative correlations during MJJAS cover both land and ocean roughly from 30°N to 70°N during the warm season as this latitude belt reacts similar to tropical land areas. During NDJFM, the negative correlation shrinks to a smaller area and mostly over land except in the North Atlantic. Positive correlation covers large areas north of 50°N during this cold season as warmer years are associated with greater moisture.

[14] Given the different spatial patterns of precipitation and temperature variations (Figure 1), it is necessary to further examine their interannual relationships in the context of large-area means. Here we focus on the global means and the means in the Tropics (25°S–25°N) where the most intense precipitation changes occur. To limit high-frequency noise, annual mean values are used. The possible linear changes in the time series will be discussed in the next subsection.

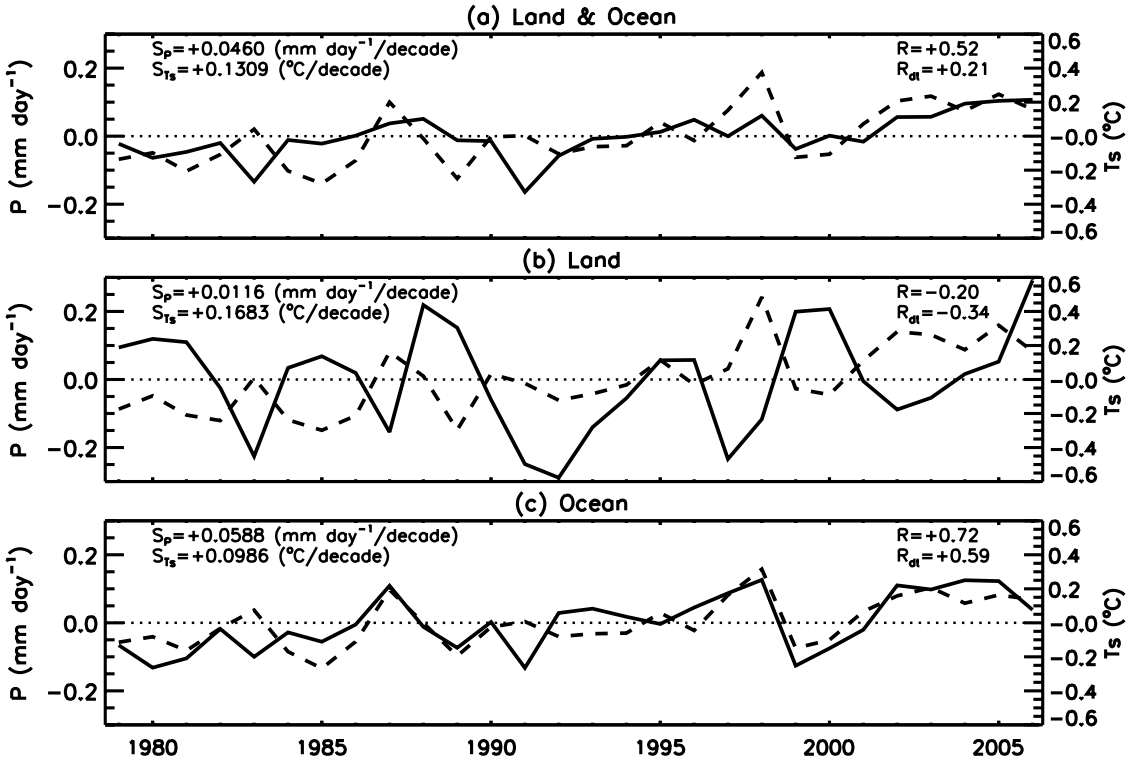

Figure 4. Same as in Figure 3 but in the Tropics (25°S–25°N).

[15] For the global totals (Figure 3a), positive correlation is found only marginally significant, and not after the same-sign linear fits are removed. Over land (Figure 3b), the interannual correlation is not significant. However, strong positive correlation is seen over the global ocean (Figure 3c). The correlation coefficient reaches the 1% confidence level, though it becomes weaker with the linear fits removed.

[16] In the Tropics, a significant, positive correlation exists between the tropical total precipitation and temperature (Figure 4a). However, after the same-sign long-term linear fits are removed, their correlation falls below the 5% confidence level, indicating a strong contribution from long-term change. For land precipitation (Figure 4b), the correlation is negative and not statistically significant with or without the effect of long-term change. As expected, strong correlation exists between precipitation and temperature over the tropical ocean (Figure 4c). Even without the contributions from the long-term linear changes existing in both components, the correlation is still well above the 1% confidence level.

[17] It is a little surprising to find a weak correlation between precipitation and temperature over tropical land in that these two variables should be dominated by the ENSO impact at the interannual timescale [e.g., *Trenberth et al.*, 1998; *Wigley*, 2000; *Gu et al.*, 2007]. We thus suspect this weak correlation may be caused by the effect of the two major volcanic eruptions during the GPCP record (El Chichón, March 1982; Pinatubo, June 1991). Previous studies showed their effective modulation of both precipitation and temperature especially in the Tropics [e.g., *Wigley*, 2000; *Soden et al.*, 2002; *Gu et al.*, 2007]. Also, these two eruptions occurred almost simultaneously with two intense El Niño events [e.g., *Gu et al.*, 2007]. Thus linear regression procedures as in *Gu et al.* [2007] are applied to isolate the effects of ENSO and volcanic eruptions, and then to further assess their impact on the relationship between precipitation and temperature. (As in *Gu et al.* [2007], Nino 3.4 and stratospheric aerosol optical thickness (τ) are used to represent the activities of these two phenomena. The entire data record is first separated into two periods based on a threshold defined by τ: $\tau \geq 0.02$ for the volcanic period and $\tau < 0.02$ for the no volcanic period. Linear relations with ENSO during the no volcanic period are then estimated for both precipitation and temperature over land and ocean separately. These relations are further applied to the volcanic period. Here we assume that the ENSO effect does not vary much during the two periods. Also, the volcanic impact is supposed to be dominant during the volcanic period after the ENSO effect is removed (linear regression indicates that it is really the case; not shown). Thus the relations with τ are estimated for precipitation and temperature separately by means of linear regression. Finally, the linear responses of both precipitation and temperature over land and ocean to ENSO and volcanic eruptions can be separately estimated.) Without the volcanic effect, the magnitudes of the correlations over both land and ocean increase (not shown). In particular, the correlation coefficient over land becomes −0.47, above the 5% confidence level. Furthermore, it becomes −0.56 with the linear fits are removed, above the 1% confidence level.

3.2. Zonal-Mean Features of Interannual Variations

[18] The relationships between precipitation and temperature are further examined in a zonal-mean sense. Linear correlations are estimated for zonal-mean monthly precipi-

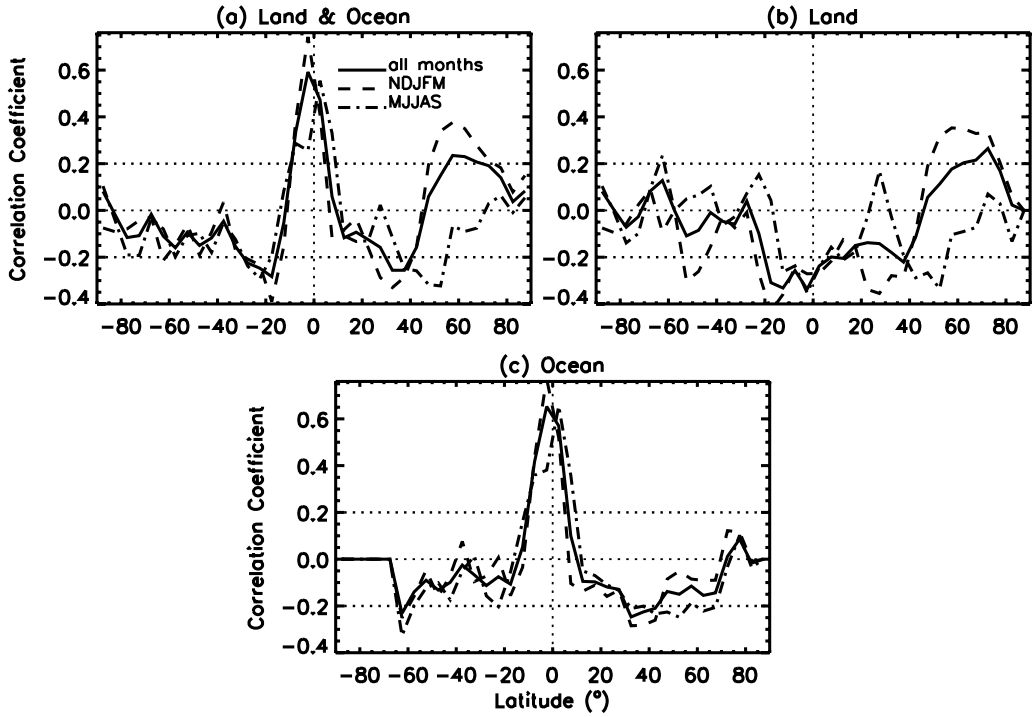

Figure 5. Correlations between zonal-mean monthly precipitation and temperature anomalies over (a) land and ocean, (b) land, and (c) ocean during all months (solid), NDJFM (dashed), and MJJAS (dash-dot). The local 5% confidence levels are about ±0.20.

tation and temperature anomalies over land & ocean, ocean, and land, respectively (Figure 5). As expected, the linear fits for the two variables have no significant impact on the gross meridional features of correlation (not shown) and are not removed for this analysis.

[19] For zonal mean totals (land & ocean, Figure 5a), strong positive correlations are observed in the deep Tropics approximately from 10°S–10°N with a maximum slightly in the Southern Hemisphere. Away from the equator, two strong negative correlation zones are located in the subtropical regions in both hemispheres: one peaks around 35°N, another 20°S. South of 35°S, the correlation is generally weak. In the Northern Hemisphere, another strong positive correlation zone is seen between about 55°N and 80°N.

[20] Examining the correlations separately for land and ocean (Figures 5b and 5c) helps elucidate how each area contributes to the total. From Figure 5c (ocean), one can see that in the deep Tropics the ocean dominates. Away from the deep Tropics, things are totally different. The negative peaks in correlation in the subtropics, although barely significant (Figure 5a, solid line), are a mixture of land and ocean contributions, which are both negative in the Northern Hemisphere. The positive correlation feature in the Northern Hemisphere at high latitudes (Figure 5a) is mainly due to land effects (Figure 5c). South of about 20°S, the correlation becomes weakly negative over ocean and near zero over land. It thus seems that the zonal mean correlations between interannual precipitation and temperature anomalies are generally controlled by the ocean in the deep Tropics. Away from the deep tropical region, the impact from ocean and land is mixed. The land surface impact may even become dominant in some regions, for instance, in the Northern Hemisphere higher latitudes, though oceanic precipitation is much stronger than over land (Figure 6). Also, compared with the meridional profile of zonal mean precipitation (Figure 6), it is interesting to note that these maximum correlation bands tend to be along the margins of the major rainfall zones. This suggests that the correlation relationships in these regions might be modulated by a few large-scale factors, not just simple regional associations between temperature and precipitation.

[21] Seasonal variations of precipitation-temperature correlations are also computed for months during NDJFM and MJJAS and displayed in Figure 5. In the Tropics and Southern Hemisphere, seasonal variation is weak, though the peak in the deep Tropics shifts from 5°S during NDJFM to 5°N during MJJAS. Evident seasonal changes in correlation are seen in the Northern Hemisphere mid-high latitudes. During NDJFM strong positive correlations exist roughly between 45°N and 80°N. During MJJAS, however, the positive correlation zone in the higher latitudes disappears, and the high negative correlation zone in the extratropics shifts northward to about 30–55°N. These seasonal changes, mainly over land, are probably related to the generally warmer temperatures and lower relative humidity values of the MJJAS season being similar to the processes which induce the negative correlations over tropical land areas. It is also interesting to note that the correlation features for all months are generally the same as NDJFM, showing the dominance of the variations of this season.

[22] Because ENSO is clearly an important factor in these variations, and to explore possible influences of the AO,

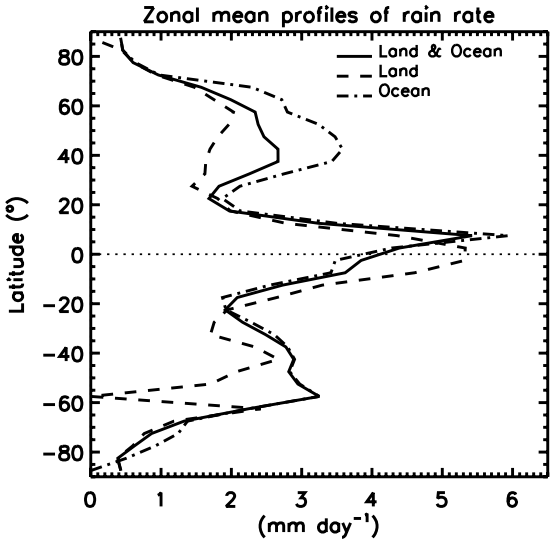

Figure 6. Meridional profiles of zonal mean monthly rain rates during 1979–2006.

especially with regard to seasonal transitions, correlations of zonal-mean precipitation and temperature anomalies with the ENSO index (Nino3.4) and the AO index, respectively, are estimated for all months, NDJFM, and MJJAS (Figure 7). Except within the deep Tropics (about 10°S–10°N) where both precipitation and temperature are positively correlated with Nino3.4, the influence of ENSO on these two variables is in opposite directions. In particular, a strong negative correlation between precipitation and Nino3.4 is observed between −10–25°S and 10–20°N, while temperature anomalies are highly, positively correlated with Nino3.4 within the same latitudinal bands. This opposing correlation feature suggests that the correlation relationships between precipitation and temperature shown earlier (Figure 5), especially in the Tropics, are heavily modulated by the ENSO events. These zonal-averaged features are also made up of land-ocean differences along latitude bands, where the ocean dominates at low latitudes and land dominates in the negative correlation zones (Figure 2).

[23] The most prominent correlations of precipitation and temperature with AO are, as expected, within the Northern Hemisphere (Figure 7). A high value of the AO index is associated with a stronger meridional temperature gradient from middle to high latitudes in the Northern Hemisphere, with the peak in zonally averaged precipitation occurring

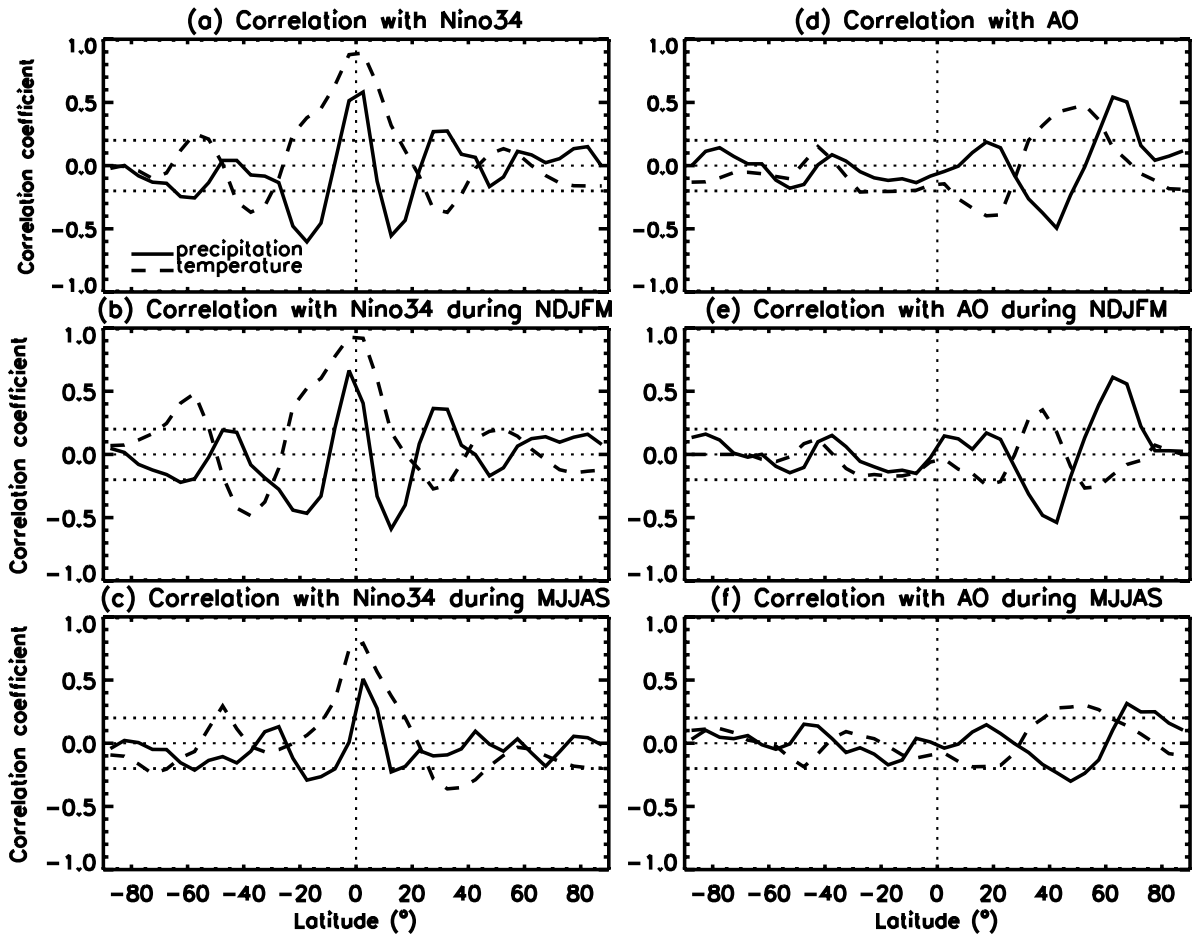

Figure 7. Simultaneous correlations of zonal-mean monthly rainfall (solid lines) and temperature (dashed lines) anomalies with the ENSO index (a, b, c), and the Arctic Oscillation index (d, e, f). The local 5% confidence levels are about ±0.20.

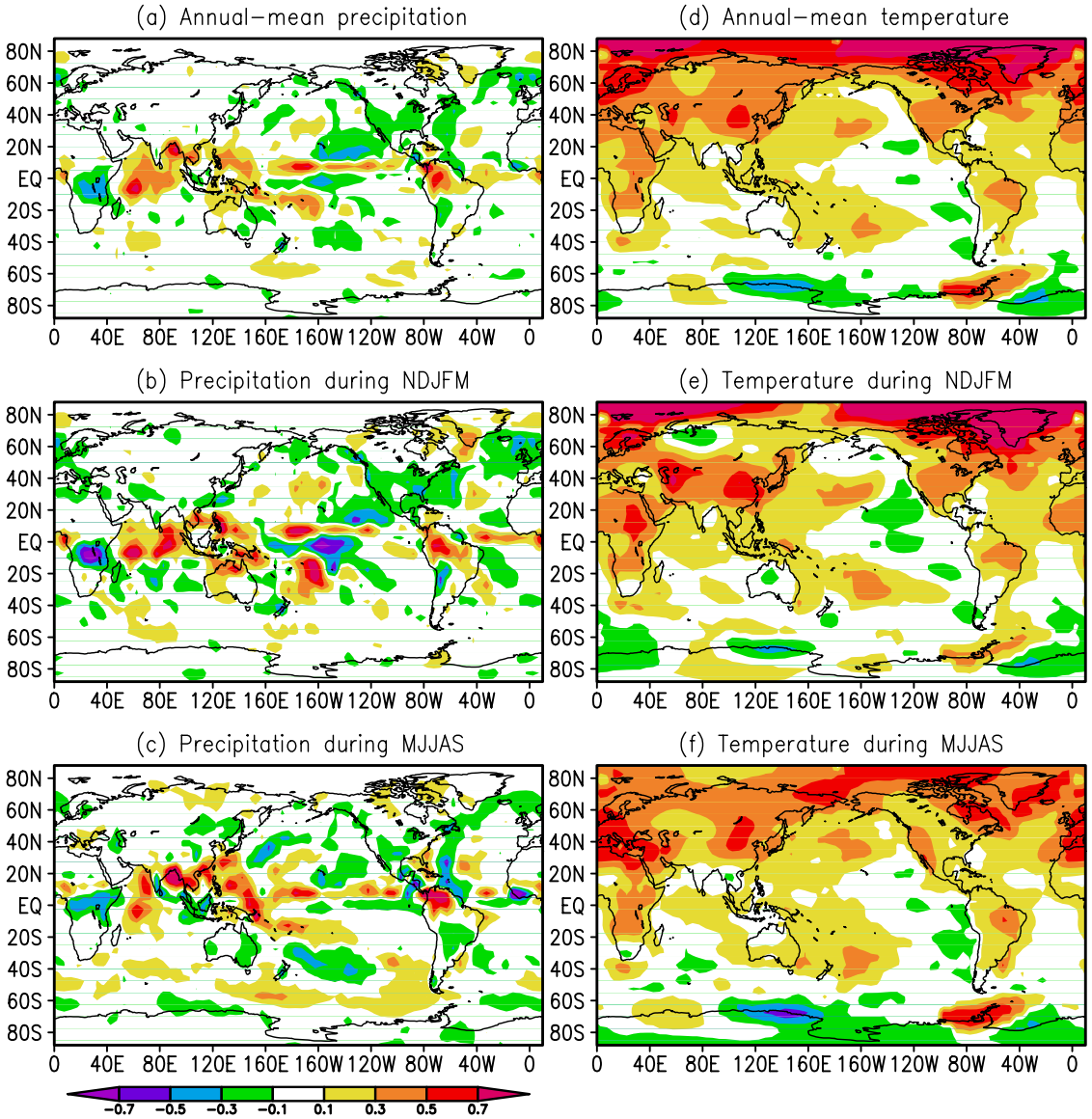

Figure 8. Linear changes in precipitation (mm day^{-1}/decade; a, b, c) and surface temperature (°C/decade; d, e, f) anomalies during 1979–2006. (a) and (d) are for the annual-means, (b) and (e) for the means during NDJFM, and (c) and (f) for the means during MJJAS.

farther poleward. The correlation between AO and precipitation tends to be opposite from that between AO and temperature except along the latitudes near 60°N. These opposite correlations may contribute to the strong negative correlation between precipitation and temperature anomalies in the Northern Hemisphere midlatitudes (25–45°N; Figure 5). On the other hand, the positive correlation of precipitation and temperature with AO occurring at about 50–65°N, specifically during NDJFM, seems to be a major contributor to the positive correlation between precipitation and temperature at the same latitudes.

[24] Therefore the correlation relationship including its seasonal variations between precipitation and temperature anomalies could be effectively controlled by the ENSO and AO, specifically in the Tropics and in the Northern Hemisphere. ENSO dominates the Tropics and extends its impact to the extratropics; AO controls the Northern Hemisphere higher latitudes and is also able to affect the tropical portion in the Northern Hemisphere.

3.3. Precipitation and Temperature Changes on the Interdecadal/Longer Timescale

[25] Previous studies showed that the atmospheric water vapor content tends to follow changes in temperature roughly obeying the Clausius-Clapeyron (C-C) relation [e.g., *Boer*, 1993; *Trenberth et al.*, 2005; *Dai*, 2006; *Held and Soden*, 2006]. However, precipitation changes may be much slower than implied by this C-C scaling based on the GCM outputs and limited observational studies [e.g., *Allen and Ingram*, 2002; *Held and Soden*, 2006; *Déry and Wood*, 2005]. Here we will look for any detectable, coherent change in precipitation and temperature on the interdeca-

Table 1. Linear Changes in the Annual-Mean Precipitation (mm day^{-1}/decade) During 1979–2006[a]

	Land and Ocean	Land	Ocean
90°S–90°N	+0.0105 (<90%)	−0.0123 (<90%)	+0.0211 (90%)
25°S–25°N	+0.0460 (97.5%)	+0.0116 (<90%)	+0.0588 (99%)

[a]The significance levels are in parentheses.

dal/longer timescales by means of these two model-independent data sets. We will then compare our results on the longer term to those already derived for the interannual scale. The linear change fits at each grid are computed for precipitation and temperature anomalies, respectively during 1979–2006 (Figure 8). To limit high-frequency noise, annual-mean and seasonal-mean values are applied. Evident contrasts exist in the linear changes for these two components. For precipitation the intense changes tend to be concentrated in the tropics with much weaker changes in the mid-higher latitudes. For surface temperature however, the intense changes occur preferentially in the regions over land and far away from the equator, with particularly strong warming appearing in the Northern Hemisphere mid-higher latitudes, manifesting the so-called "Polar Amplification" [e.g., *Pierrehumbert*, 2002]. This contrasting feature is in general similar to the spatial distributions of their respective standard deviations (Figure 1), despite the standard deviations primarily reflecting their interannual variability.

[26] The spatial pattern of precipitation changes is generally consistent with that reported in *Smith et al.* [2006]. There is an upward increase in the tropical Atlantic and Indian Oceans. In the Pacific, a band of precipitation increase is seen roughly along the mean latitude of the ITCZ, but sandwiched by two bands of precipitation reduction south and north of it in the tropical central-eastern Pacific. A precipitation increase can also be seen along the South Pacific Convergence Zone (SPCZ) and over tropical South America. Over the central African continent a zone of precipitation reduction exists. Seasonal differences for precipitation changes are evident in several regions. In the tropical central Pacific, the changes are stronger during NDJFM. Seasonal reversal even seems to exist in the tropical Atlantic with positive (negative) changes along the equator during NDJFM (MJJAS). In the mid-higher latitudes, more intense changes are seen during NDJFM (MJJAS) for the Northern (Southern) Hemisphere.

[27] For temperature changes, large warming covers the areas in the Northern Hemisphere higher latitudes [e.g., *Hansen et al.*, 1999; *Simmons et al.*, 2004]. In the lower-latitudes, the largest temperature changes are focused over land. However, over the Pacific Ocean broad, weak maxima are apparent at 30°N and 30°S, with a relative minimum located along the equator and a cooling in the central-eastern Pacific region covering the ENSO activity zone [e.g., *Cane et al.*, 1997]. The amplitudes of change vary with season in several regions.

[28] Linear change values of precipitation over the 27-year period for the globe and Tropics (and their significance level) are given in Table 1 (see also Figures 3 and 4). The significance levels of these changes are estimated based on the two-tailed t test after accounting the temporal autocorrelations in the residual time series [e.g., *Livezey and Chen*, 1983; *Chu and Wang*, 1997; *Santer et al.*, 2000]. Over the global ocean the small precipitation increase is significant, but only at the 90% level. The combined land and ocean change is not significant and the slight decrease calculated over global land is also not significant. In the Tropics, however, the land and ocean combined has a significant slope, as does the ocean alone, as was previously noted by *Gu et al.* [2007] for a 1-year shorter GPCP record. On the other hand, positive linear changes of surface temperature during the same 27-year period for both the globe and Tropics are significant at the 99% level (Figures 3 and 4).

[29] Zonal-mean profiles of linear change for both variables are further estimated (Figure 9). For the total precipitation (solid line in Figure 9a), the largest change occurs in the deep Tropics with precipitation increase observed roughly from 20°S–20°N and peaking along the center of the time-mean ITCZ. The peak rate of change at 5–10°N is statistically significant at the local 95% level; the linear

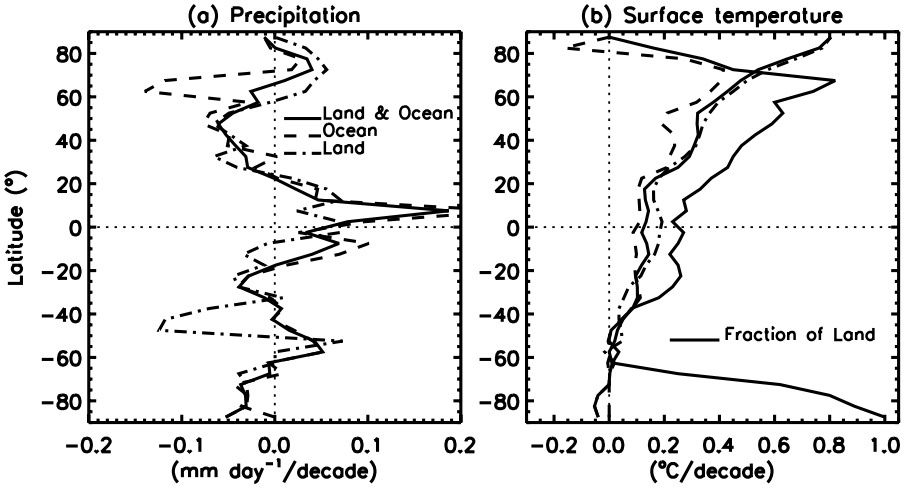

Figure 9. Long-term linear changes in zonal-mean, annual (a) rainfall and (b) surface temperature anomalies as function of latitude. Also shown in b is the fraction coverage of land.

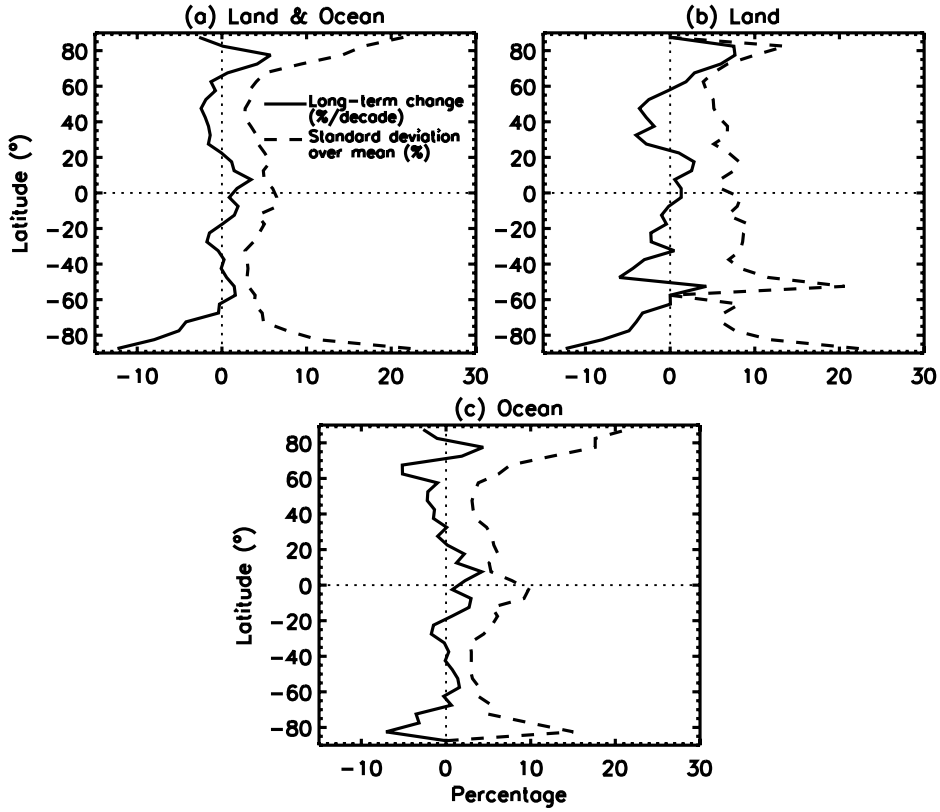

Figure 10. Relative long-term precipitation changes (%/decade; solid lines) and the ratios (%; dashed lines) between standard deviations and zonal mean rain rates over (a) land and ocean, (b) land, and (c) ocean.

change over the full 25°N–25°S zone (Table 1) is significant at the local 97.5% level. In the Northern Hemisphere extratropics and higher latitudes, a band of precipitation reduction extends from 20–65°N, while from 65–80°N a precipitation increase is seen. The peak negative change at 45–50°N is also statistically significant at the local 95% level; however, the high latitude peak in the diagram is not significant at that level. The quality and homogeneity of the precipitation information at that high latitude is also suspect. In the Southern Hemisphere, precipitation increases are seen in the data set from 45–65°S, whereas precipitation reduction is observed at two latitude bands: 20–35°S and south of 70°S. However, none of these Southern Hemisphere features are statistically significant at the local 95% level and interpretation of these features should be made with caution. Between oceanic and land precipitation, some differences are observed (Figure 9a). Positive changes for land precipitation are weaker in the Tropics. Particularly, negative changes can be found between 5°S and 20°S, likely corresponding to the precipitation reduction in tropical central Africa (Figure 8). When the long-term zonal-mean precipitation change is examined in terms of percentage (solid lines in Figure 10), the tropical peak at 3% per decade is no longer dominant. In fact, all the maxima and minima have an absolute value of 2–5% per decade, except over Antarctica. One should keep in mind the previous discussion of the local statistical significance of the peaks and valleys of precipitation change and focus on the Tropics and subtropics and interpret and compare the features at other latitudes carefully. The accuracy of the precipitation data and analysis over Antarctica, for example, is suspect, but it is interesting that this is the only location where the surface temperature data set shows a long-term decrease (Figure 9b). As expected the linear changes for the zonal-mean temperature show a totally different pattern (Figure 9b). There is a gradual, northward increase for the total, oceanic, and land surface temperature prior to reaching the latitude of about 70°N. North of it, the impact of ocean ice could be significant. Interestingly, this northward temperature increase roughly follows the increase of land surface coverage except near the two polar zones. This tends to confirm that temperature might be more sensitive or changeable over land given much larger oceanic thermal inertia

3.4. Long-Term Precipitation-Temperature Change Ratios

[30] The long-term ratios of precipitation change to temperature change are, of course, of interest in attempting to understand the global system. On the global scale, Table 2 indicates the ratios calculated for the globe and for the Tropics for the 1979–2006 period. There are upward increases for both precipitation and temperature (Figure 3a and Table 1) on the global scale, resulting in a ratio of +0.06 mm day^{-1}/°C or +2.3%/°C), much smaller than implied by the C-C scaling, but interestingly being of the same order as modeling outputs [e.g., *Allen and Ingram*,

Table 2. Ratios Between Linear Changes in the Annual-Mean Precipitation and Surface Temperature Anomalies (mm day^{-1}/°C) During 1979–2006[a]

	Land and Ocean	Land	Ocean
90°S–90°N	+0.0602 (+2.3)	−0.0589 (−2.8)	+0.1896 (+6.3)
25°S–25°N	+0.3514 (+11.3)	+0.0689 (+2.2)	+0.5963 (+19.3)

[a]The relative values (%/°C) evaluated by the corresponding mean rain rates are in parentheses.

2002; *Held and Soden*, 2006]. However, the global precipitation change in the GPCP data set is very small (and not statistically significant at the 95% level), and considering the nonhomogeneous nature of the data set and other data factors, we are very cautious about the accuracy of this calculation. Recently, *Wentz et al.* [2007] performed a similar calculation for a shorter period (1988–2006) and arrived at a larger value (+6%/°C), even though they used GPCP analysis for the over-land portion of their input and to calibrate their ocean mean value. If we limit our calculation to the same period we arrive at a very similar value. The end result of these global precipitation-temperature slope calculations is a probable positive value, but with a magnitude that is very sensitive to the length of record and the data quality in terms of precipitation change signal.

[31] It is interesting, however, to also look at subglobal regions. In Table 2 global ocean has a relatively large value (+6%/°C), while global land has a small negative value (−3%/°C), pointing to possibly very different processes over ocean and land. Restricting the area to the Tropics also changes the numbers, with total tropics (land plus ocean) having a ratio of +11%/°C, and with ocean alone having an even larger ratio of long-term change. Figure 11 shows the latitudinal distribution of the ratio between precipitation and surface changes for ocean, land and combined. Due to the uncertainty of data sets and the extreme large values south of 40°S caused by relatively large precipitation changes and negligible temperature changes (Figure 9), meridional profiles are only shown from 40°S–90°N. It is not surprising that the meridional profiles of the long-term ratios closely follow those for the precipitation changes, and that the largest values are generally seen in the Tropics. The ratios in the Northern Hemisphere are small simply because of large temperature changes and relatively small precipitation changes. It is obvious that the global ratio value of precipitation change to temperature change reflects an integration of highly variable regional values and therefore an integration over very different regional precipitation processes.

3.5. Interannual Ratio Changes and Comparison to Long-Term Changes

[32] The long-term changes calculated in the last section, both globally and regionally, require detection of relatively small precipitation signals. *Gu et al.* [2007] have explored the limits of that detection and concluded that the tropical precipitation signals are real. At higher latitudes the signal is smaller, although perhaps not fractionally, and there are greater questions regarding the retrieval and analysis techniques. However, at the interannual scale the precipitation (and surface temperature) signals are larger and robust, at least regionally (Figure 1). In Figure 10 the shapes of the interannual, zonally averaged precipitation variability (dashed lines) show some similarity in shape to the long-term change percentages.

[33] One might expect that temperature-precipitation relations at the interannual scale would also have some similarities and some differences with those relations at a longer (interdecadal) timescale. For the interannual scale Table 3 shows global, ocean and land totals, with the global total value for interannual variability similar to that of the long-term change (Table 2). Interannual and long-term changes are also similar over the ocean for both the globe and Tropics. However, over land there is a distinct disparity between the two time regimes, indicating the ENSO impact on the interannual changes. The latitudinal profile of the ratios (both interannual and long-term) in Figure 11a (and Figure 12a for the percentage change) shows a similarity in the relations for ocean and land combined with both having a near-equatorial peak and negative values at subtropic latitudes. There are also secondary maxima at higher latitudes (40–70°N). The separation into land and ocean (Figures 12b and 12c) indicates that the global profile is dominated by the ocean and that the ocean profiles are similar, both in the Tropics and higher latitudes. However, the land profiles are distinctly different in the Tropics, clearly drawing a distinction between ENSO processes at the interannual timescale in the Tropics and other processes at the longer timescale. The interannual peak in the Tropics, however, is narrower than the long-term change there going negative at 10°N and 10°S, instead of 20°N and 20°S, both over ocean and ocean & land combined. Just as the ENSO interannual process varying zonally, it is also different from the long-term process latitude-wise. This is possibly related to strengthening of the Hadley circulation during El Nino (interannual warming event), but a broader north-south circulation variation with long-term warming. The meridional shift continues into midlatitudes with the long-term minimum poleward of the interannual minimum in both hemispheres. Therefore except for the tropical land areas there is a general similarity between the two timescales in terms of this precipitation-temperature parameter, but the width and latitude location of the features show variation. These results may indicate that the processes governing the long-term relations are also at work to a certain extent in a similar fashion at the interannual scale, but with significant, measurable differences.

[34] The general similarity also may give more credence to the long-term relations derived from the precipitation data set. The precipitation analysis is on strong ground on the regional, interannual time/space scale. Seeing similar pat-

Table 3. Regression Coefficients (mm day^{-1}/°C) of the Annual-Mean Precipitation Anomalies Against Surface Temperature Anomalies[a]

	Land & Ocean	Land	Ocean
90°S–90°N	+0.1018 (+3.9)	+0.1326 (+6.3)	+0.2695 (+9.4)
25°S–25°N	+0.0839 (+2.7)	−0.3648 (−11.4)	+0.3355 (+10.9)

[a]The relative values (%/°C) evaluated by the corresponding mean rain rates are in parentheses. Long-term linear changes are removed for both variables.

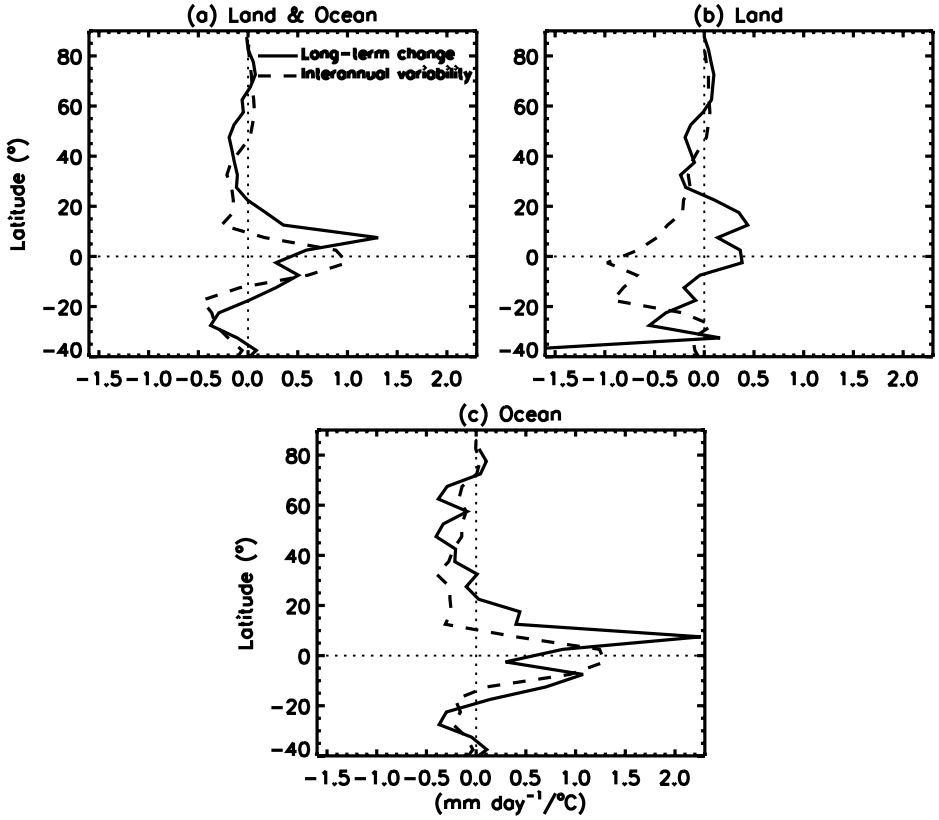

Figure 11. Meridional profiles of the ratios between precipitation and surface temperature changes on the long-term (solid lines) and interannual (dashed lines) timescales over (a) land and ocean, (b) land, and (c) ocean.

terns and magnitudes on both timescales gives support to the analysis at the longer timescale. However, much more work is required in analyzing the data sets and comparing these types of parameters with model results to describe the causes for the variations and understand quantitatively the precipitation-temperature relations. The relative change in relative humidity heavily depends on the relative fluctuations in both temperature and specific humidity.

[35] So the actual moisture, and presumably precipitation change is determined by both the temperature and specific humidity changes. If there is a balance between the changes in temperature and humidity as shown in model outputs on a global scale [e.g., *Allen and Ingram*, 2002; *Held and Soden*, 2006], precipitation should not vary much. However, these relations must also be felt to some degree over large regional areas. For regional means, various change rates can be found likely due to the imbalance of energy and water resource as can be see clearly from the latitudinal profiles.

4. Summary and Concluding Remarks

[36] Global and large regional rainfall and surface temperature changes, and their possible relations on interannual and interdecadal/longer timescales are examined by means of two model-independent data sets: the 28-year (1979–2006) GPCP monthly data set and the NASA-GISS surface temperature anomaly product.

[37] At the interannual timescale, linear correlations between these two variables are estimated to quantify their possible relationship across the globe. In the Tropics, positive (negative) correlations are generally observed over oceans (lands). ENSO tends to dominate these interannual, tropical relations. In the Southern Hemisphere mid-higher latitudes, the correlation is relatively weak. In the Northern Hemisphere mid-higher latitudes, this correlation relationship becomes strong and complicated with positive and negative values of correlation being able to occur over both ocean and land. Both ENSO and AO modulate this relationship north of the equator. In particular, a strong seasonal shift in the correlation relation tends to occur in the Northern Hemisphere higher latitudes, likely manifesting the seasonal modulation of AO. Thus the linear correlations between these two variables indicate both regional interactions between precipitation and surface temperature, and the remote modulations of large-scale circulation anomalies.

[38] On the interdecadal/longer timescale, the relationships between precipitation and surface temperature are examined by estimating and further comparing their linear fits during the GPCP record. The most intense long-term, linear changes in precipitation are within the Tropics along with the largest interannual rainfall variances. On the other hand, the strongest linear changes and largest variances for surface temperature appear in the Northern Hemisphere mid-high latitudes. In the Tropics and Southern Hemisphere, temperature change is much weaker. This meridional feature of variation is likely related to the northward

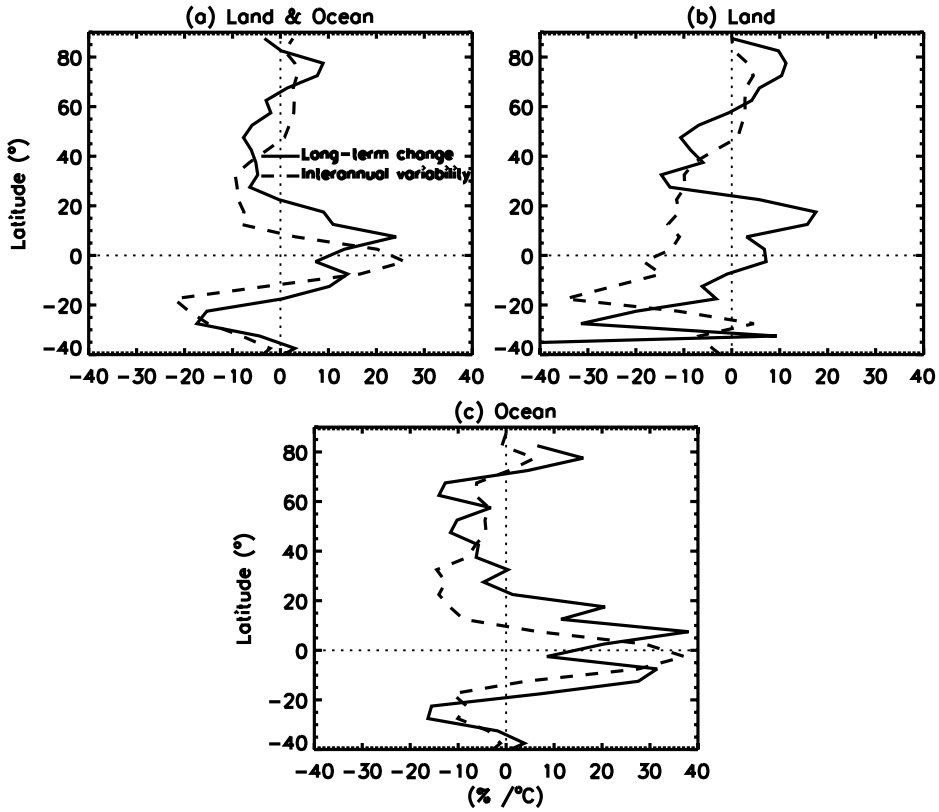

Figure 12. Relative values of the ratios between precipitation and surface temperature changes on the long-term (%/C per decade; solid lines) and interannual (%/C per decade; dashed lines) timescales over (a) land and ocean, (b) land, and (c) ocean.

increase of land surface fraction coverage, except in the two polar regions.

[39] The ratios between the long-term linear changes in zonal-mean rainfall and temperature over the GPCP data period are estimated, with the change rate for the global total precipitation against the global mean temperature change showing a moderate positive number (+2.3%/°C), roughly in agreement with previous modeling results [e.g., *Allen and Ingram*, 2002; *Held and Soden*, 2006]. However, this number is sensitive to the period examined, with a larger value calculated for the shorter 1988–2006 period [*Wentz et al.*, 2007]. Finally, comparing the long-term precipitation-temperature change ratios to those at the interannual scale shows a similarity in the relations for ocean and land combined, with both having a near-equatorial peak and negative values at subtropic to middle latitudes. The ocean profiles are very similar at the two time resolutions, but the land profiles are distinctly different in the Tropics, clearly pointing to the ENSO processes at the interannual timescale in the Tropics. The interannual peak in the Tropics, however, is narrower than the long-term change there, both over ocean and ocean & land combined. This difference may be related to strengthening of the Hadley circulation during a warm, El Nino event, but a broader or weakening north-south circulation variation with long-term warming. The long-term change minima of the subtropical to midlatitude zone are located poleward of the interannual minima in both hemispheres. However, the general similarity between the profiles, except for the tropical land areas, indicates an overlap of controlling processes between the two timescales in terms of this precipitation-temperature parameter, but with the width and latitude location of the features showing variation. The similarity also may indirectly support conclusions as to long-term relations derived from the GPCP precipitation data set. It is hoped that this type of analysis will be useful in eventually understanding the temperature-precipitation linkages in the global system. Joint analysis with global model results along these lines will help to diagnose the relationships and evaluate the utility of the model calculations.

[40] **Acknowledgments.** The global surface temperature anomaly product and global mean stratospheric aerosol optical thickness data were provided by the NASA-GISS from its website at http://data.giss.nasa.gov/. This research is supported under the NASA Energy and Water-cycle Study (NEWS) program.

References

Adler, R. F., et al. (2003), The version 2 Global Precipitation Climatology Project (GPCP) monthly precipitation analysis (1979–present), *J. Hydrometeorol.*, *4*, 1147–1167.

Allan, R. P., and B. J. Soden (2007), Large discrepancy between observed and simulated precipitation trends in the ascending and descending branches of the tropical circulation, *Geophys. Res. Lett.*, *34*, L18705, doi:10.1029/2007GL031460.

Allen, M. R., and W. J. Ingram (2002), Constraints on future changes in climate and the hydrologic cycle, *Nature*, *419*, 224–232.

Boer, G. J. (1993), Climate change and the regulation of the surface moisture and energy budgets, *Clim. Dyn.*, *8*, 225–239.

Cane, M. A., A. C. Clement, A. Kaplan, Y. Kushnir, D. Pozdnyakov, R. Seager, S. E. Zebiak, and R. Murtugudde (1997), Twentieth-century sea surface temperature trends, *Science*, *275*, 957–960.

Chu, P.-S., and J.-B. Wang (1997), Recent climate change in the tropical western Pacific and Indian ocean regions as detected by outgoing longwave radiation records, *J. Clim.*, *10*, 636–646.

Curtis, S., and R. F. Adler (2003), The evolution of El Niño-precipitation relationships from satellites and gauges, *J. Geophys. Res.*, *108*(D4), 4153, doi:10.1029/2002JD002690.

Dai, A. (2006), Precipitation characteristics in eighteen coupled climate models, *J. Clim.*, *19*, 4605–4630.

Dai, A., and T. M. L. Wigley (2000), Global patterns of ENSO-induced precipitation, *Geophys. Res. Lett.*, *27*, 1283–1286.

Dai, A., I. Y. Fung, and A. D. Del Genio (1997), Surface observed global land precipitation variations during 1900–88, *J. Clim.*, *10*, 2943–2962.

Déry, S. J., and E. F. Wood (2005), Observed twentieth century land surface air temperature and precipitation covariability, *Geophys. Res. Lett.*, *32*, L21414, doi:10.1029/2005GL024234.

Gillett, N. P., A. J. Weaver, F. W. Zwiers, and M. F. Wehner (2004), Detection of volcanic influence on global precipitation, *Geophys. Res. Lett.*, *31*, L12217, doi:10.1029/2004GL020044.

Gu, G., R. F. Adler, G. Huffman, and S. Curtis (2007), Tropical rainfall variability on interannual-to-interdecadal/longer-timescales derived from the GPCP monthly product, *J. Clim.*, *20*, 4033–4046.

Hansen, J., R. Ruedy, J. Glascoe, and M. Sato (1999), GISS analysis of surface temperature change, *J. Geophys. Res.*, *104*, 30,997–31,022.

Held, I., and B. Soden (2006), Robust responses of the hydrological cycle to global warming, *J. Clim.*, *19*, 5686–5699.

IPCC, Climate Change (2007), The physical science basis, in *Contribution of Working Group 1 to the Fourth Assessment Report of the Intergovernmental Panel on Climate Change*, p. 996, Cambridge University Press, Cambridge, U.K.

Isaac, G. A., and R. A. Stuart (1992), Temperature-precipitation relationships for Canadian stations, *J. Clim.*, *5*, 822–830.

Kumar, A., F. Yang, L. Goddard, and S. Schubert (2004), Differing trends in the tropical surface temperatures and precipitation over land and oceans, *J. Clim.*, *17*, 653–664.

Livezey, R. E., and W. Y. Chen (1983), Statistical field significance and its determination by Monte Carlo techniques, *Mon. Weather Rev.*, *111*, 46–59.

Madden, R. A., and J. Williams (1978), The correlation between temperature and precipitation in the United States and Europe, *Mon. Weather Rev.*, *106*, 142–147.

Mantua, N. J., and S. R. Hare (2002), The Pacific decadal oscillation, *J. Oceanogr.*, *58*, 35–44.

Pierrehumbert, R. T. (2002), The hydrologic cycle in deep-time climate problems, *Nature*, *419*, 191–198.

Rasmusson, E. M., and T. H. Carpenter (1982), Variations in tropical sea surface temperature and surface wind fields associated with the Southern Oscillation/El Niño, *Mon. Weather Rev.*, *110*, 354–384.

Reynolds, R. W., N. A. Rayner, T. M. Smith, D. C. Stokes, and W. Wang (2002), An improved in situ and satellite SST analysis for climate, *J. Clim.*, *15*, 1609–1625.

Robock, A. (2000), Volcanic eruptions and climate, *Rev. Geophys.*, *38*, 191–219.

Santer, B. D., T. M. L. Wigley, J. S. Boyle, D. J. Gaffen, J. J. Hnilo, D. Nychka, D. E. Parker, and K. E. Taylor (2000), Statistical significance of trends and trend differences in layer-average atmospheric temperature time series, *J. Geophys. Res.*, *105*(D6), 7337–7356.

Simmons, A. J., et al. (2004), Comparison of trends and low-frequency variability in CRU, ERA-40, and NCEP/NCAR analyses of surface air temperature, *J. Geophys. Res.*, *109*, D24115, doi:10.1029/2004JD005306.

Smith, T. M., X. Yin, and A. Gruber (2006), variations in annual global precipitation (1979–2004), based on the Global Precipitation Climatology Project 2.5° analysis, *Geophys. Res. Lett.*, *33*, L06705, doi:10.1029/2005GL025393.

Soden, B. J., R. T. Wetherald, G. L. Stenchikov, and A. Robock (2002), Global cooling after the eruption of Mount Pinatubo: A test of climate feedback by water vapor, *Science*, *296*, 727–730.

Thompson, D. W. J., and J. M. Wallace (1998), The Arctic Oscillation signature in the wintertime geopotential height and temperature fields, *Geophys. Res. Lett.*, *25*, 1297–1300.

Trenberth, K. E., and D. J. Shea (2005), Relationship between precipitation and surface temperature, *Geophys. Res. Lett.*, *32*, L14703, doi:10.1029/2005GL022760.

Trenberth, K. E., G. W. Branstator, D. Karoly, A. Kumar, N.-C. Lau, and C. Ropelewski (1998), Progress during TOGA in understanding and modeling global teleconnections associated with tropical sea surface temperatures, *J. Geophys. Res.*, *103*, 14,291–14,324.

Trenberth, K. E., J. M. Caron, D. P. Stepaniak, and S. Worley (2002), Evolution of El Niño-Southern Oscillation and global atmospheric surface temperatures, *J. Geophys. Res.*, *107*(D8), 4065, doi:10.1029/2000JD000298.

Trenberth, K. E., J. Fasullo, and L. Smith (2005), Trends and variability in column-integrated atmospheric water vapor, *Clim. Dyn.*, *24*, 741–758.

van Loon, H., G. A. Meehl, and J. M. Arblaster (2004), A decadal solar effect in the tropics in July–August, *J. Atmos. Sol.-Terr. Phys.*, *66*, 1767–1778.

Wentz, F. J., L. Ricciardulli, K. Hilburn, and C. Mears (2007), How much more rain will global warming bring?, *Science*, *317*, 233–235.

Wigley, T. M. L. (2000), ENSO, volcanoes and record-breaking temperatures, *Geophys. Res. Lett.*, *27*, 4101–4104.

Yang, F., A. Kumar, M. E. Schlesinger, and W. Wang (2003), Intensity of hydrological cycles in warmer climates, *J. Clim.*, *16*, 2419–2423.

Zhao, W., and M. A. K. Khalil (1993), The relationship between precipitation and temperature over the contiguous United States, *J. Clim.*, *6*, 1232–1236.

R. F. Adler, Code 613.1, NASA/GSFC, Greenbelt, MD 20771, USA. (robert.f.adler@nasa.gov)

D. Bolvin and G. J. Huffman, Science Systems and Applications Inc, Greenbelt, MD, USA.

S. Curtis, Department of Geography, East Carolina University, Greenville, NC, USA.

G. Gu and J.-J. Wang, Goddard Earth Sciences and Technology Center, University of Maryland Baltimore County, Baltimore, MD, USA.